

Microstructure and Mechanical Properties of Rotary Friction Welded IN-600 and SS316L with Copper Interlayer



Neeraj K. Mishra and Amber Shrivastava

Abstract The ability to weld Inconel with stainless steel would enable design simplification for various high-temperature applications. Fusion welding and plastic deformation-based solid-state joining techniques lead to intermetallics and significant deformation zones, leading to inferior joint performance. In this work, rotary friction welds of In-600 and SS316L are performed with and without Cu interlayer, at 3000 rpm, 10 mm/min of friction feed rate, and 60 mm/min forging feed rate. Near the joint interface, dynamic recrystallization driven grain refinement on steel side and grain coarsening on Inconel side are noticed. Tensile testing results show that the joint strength and ductility of the joints with Cu interlayer are appreciably higher than the same for the joints made without interlayer. For the joints with Cu interlayer, fractography indicates ductile fracture and EDS analysis of the fracture surface suggests uniform spreading of copper at the steel side, which would impede the formation of brittle Fe–Ni intermetallics. For joints without Cu interlayer, cleavage marks are noticed on the steel side fracture surface, with significant presence of Ni indicating Fe–Ni intermetallics, which would promote brittle fracture. The joint efficiency of the joints made with Cu interlayer is 97.5% with 25.7% elongation, which also compares decently against the same for the base material (33% for Inconel 600).

Keywords Dissimilar rotary friction welding · Interlayer · Dynamic recrystallization · IN600 · SS316L

Introduction

The joining of dissimilar materials is an area of active research, owing to several benefits it can bring to various products/applications such as cost effectiveness, light

N. K. Mishra · A. Shrivastava (✉)

Department of Mechanical Engineering, Indian Institute of Technology Bombay, Powai, Mumbai, Maharashtra 400076, India

e-mail: ashrivastava.me@iitb.ac.in

weighting, design flexibility, etc. [1]. Use of solid-state welding techniques is extensively explored for joining of dissimilar materials, particularly for the material combinations which are difficult to join with traditional fusion welding methods. Rotary friction welding (RFW) is a solid state welding process that works well for cylindrical workpieces. In this process, two parts to be welded are brought into contact, such that the contacting surfaces undergo intense frictional heating and severe plastic deformation due to the relative motion of the parts. The mechanical intermixing of materials and heat generation takes place at the interface, which enhances the diffusion between the materials due to high temperature, resulting in strong metallurgical bonds at interface [10].

Inconel, a Ni-based super-alloy, is known for its high-temperature strength. This makes it useful in many high temperature applications such as aerospace, etc. [2]. Steel, an alloy of iron and carbon, is a prevalent material used extensively for many structural applications and machine components. The components of these two materials are placed next to each other for different application areas, such as, chemical industries, aerospace industries, and geothermal power plants, etc. [3–5]. For example, in the aerospace industry, the turbine blades are made of Inconel alloy and turbine shaft is made of steel [6, 7]. Rotary friction welding can be used to make bimetallic turbine shaft of AMS 6304 stainless steel and Inconel 718 [7]. Some of the works explored the use of conventional fusion welding techniques to join Inconel and steel. Mortezaie, A. et al. [1] performed gas tungsten arc welding of Inconel 718 and 310 steel and noticed the redistribution of Niobium (Nb) and Molybdenum (Mo) upon solidification because of constitutional supercooling, which further led to preferential corrosion in the dendritic core. Ahmad et al. [8] attempted the joining of Inconel 625 and duplex stainless steel 2205 with laser beam welding. Similar to the previous work, the segregation of Nb and Mo upon solidification was observed, which promoted the failure of the welded joints. Similar studies have highlighted various challenges associated with fusion welding of Inconel and steel. Such as, the microstructure is destroyed and associated mechanical properties are lost upon fusion welding of dispersion strengthened Inconel alloys. Further the welded/solidified region is prone to defects like shrinkage cracks, large residual stresses and voids, which ultimately lead to the poor weld performance [1–8].

Some of the studies have also explored the welding of Inconel and steel using solid-state joining techniques. The maximum joint strength of 652 MPa with 22% elongation was achieved for rotary friction welded joints of Inconel 718 and stainless steel SS 410S [9]. These joints deformed and failed on the steel side due to presence of martensite. In an interesting study, the effect of choice of rotating and stationary material is shown for dissimilar RFW of different grades of Inconel (Inconel 718 and Inconel 600) [10]. Severe plastic deformation and grain coarsening were observed on Inconel 718 side placed on stationary side, though Inconel 718 possesses higher yield and ultimate tensile strength than Inconel 600 [10]. Researchers have observed intermetallic compounds (IMC) in the friction stir welds of super duplex stainless steel SAF2507 and Inconel 825 [11]. Lower joint ductility of 12% (% elongation) as compared to base material was attributed to the presence of IMCs [11]. Similarly, for inertia friction welded joints of alloy steel 42CrMo and Ni alloy K418, intermetallic

compounds like $Fe_{0.64}Ni_{0.36}$, Ni-Fe-Cr, Ni_3 (Al, Ti) were found at the joint interface. Some metal carbides (MC-type carbides) like TiC and NbC were also observed, drastically reducing the joint ductility [12]. Thus, some of the limitations/challenges with fusion welding of Inconel and steel are addressed by using solid state joining techniques. However, the formation of IMCs and their detrimental effect on the joint performance persists. So further strategies for inhibiting or reducing the IMC formation would be needed, to improve the strength and ductility for dissimilar joints of Inconel and steel. Reddy et al. used Ni interlayer between maraging steel and low alloy steel during RFW and reported improvement in hardness, impact toughness and tensile strength of the joints [13]. In another study [14], three interlayer different materials (copper, nickel, and silver) were used for the RFW of aluminum alloy AA 6061 to AISI 304 steel. The joints made using Ag interlayer exhibited the maximum strength and joints made without any interlayer exhibited the minimum strength, among all the joints. The minimum strength (of joints without interlayer) was attributed to the formation of Fe_2Al_5 brittle intermetallic. $CuAl_2$ and $NiAl_3$ IMCs were observed in the joints prepared with Cu and Ni interlayers, respectively. Silver acted as a barrier for diffusion of Fe and avoided the formation of Fe_2Al_5 , in the welds with silver interlayer. This led to significant improvement in the ductility of joint with Ag interlayer (100° bend angle) as compared against the weld without interlayer (0° bend angle). Joining of aluminium alloy (AA6061) to steel (AISI 4340) with silver interlayer was also attempted by Meshram et al. [15]. Less hard Ag-Al IMCs (as compared against Fe-Al IMCs) were noticed in the joints, which led to improvement in the ductility of the joint. Fe and Cu are immiscible, and Cu-Ni is an isomorphs system. This would allow Cu interlayer to limit the formation of detrimental intermatllics. The present work investigates the effect of Cu interlayer on the joint performance of the rotary friction welded joints of Inconel 600 and SS316L.

Experimental Methodology and Characterization

The chemical composition for the base materials are presented in Table 1. Commercially pure copper with 99.6% purity was used for the interlayer material. The 12 mm diameter rods of Inconel 600 and SS316 were rotary friction welded on three-axis LMW LV55 vertical milling center in the displacement controlled mode. A schematic and the setup of RFW are shown in Fig. 1, where *R* represents the radial direction and *Z* represents the axial direction.

Table 1 Chemical composition of base materials

Elements material	% Ni	% Cr	% Mn	% Fe	% Mo	Balance (%)
Inconel 600	72	18	0.2	9	–	<1
SS 316L	10	18	2	67	2	<1

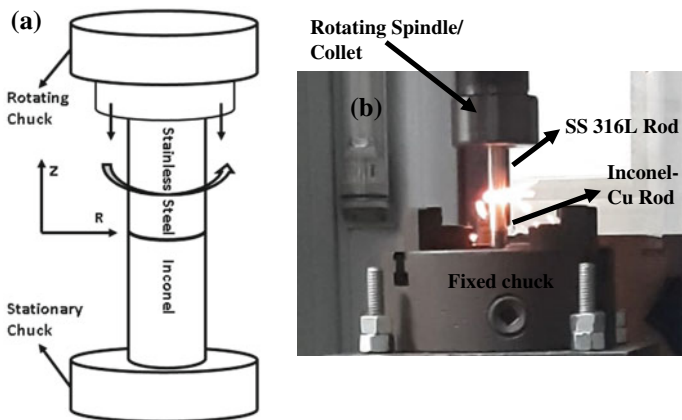


Fig. 1 a Schematic and b setup of RFW

RFW of Inconel 600 and SS 316L steel with Cu interlayer was performed in two steps. In first step, 12 mm dia. Cu rod was RFWed to the Inconel 600 rod. Cu rod was held in the rotating collet/spindle and Inconel 600 was held stationary at the chuck mounted on the CNC table. Process parameters for Cu to Inconel 600 joining are given in Table 2. The Cu-Inconel 600 joint was machined, to leave 0.8 mm (Cu interlayer thickness) of Cu with the joint (Fig. 2). In second step, SS 316L was RFWed to the Inconel 600 with Cu interlayer. The SS 316L rod was held in the rotating collet/spindle and Inconel 600 with Cu interlayer was held stationary on the CNC table (Fig. 1). Process parameters for joining of SS 316L to Inconel 600 with Cu interlayer are given in Table 2. In both the steps, the RFW process started with the rotation (at pre-determined rpm, Table 2) of the rod held in collet/spindle. Next, the rotating rod is lowered to contact the stationary rod. Upon contact, a dwell time of 5 s was allowed to remove the surface oxide layers from the work pieces by rubbing action. Then during friction stage, the rotating rod plunged into the stationary rod for

Table 2 Process parameters

Joint	RPM	Friction feed (mm/min)	Friction plunge (mm)	Forging feed (mm/min)	Forging depth (mm)
Cu to Inconel 600	2500	10	5	60	3
SS 316L to Inconel 600 with Cu interlayer	3000	10	5	60	3
SS 316L to Inconel 600 (without Cu interlayer)	3000	10	5	60	3

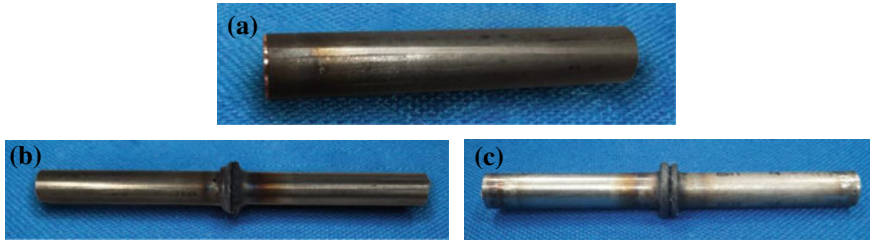


Fig. 2 a Inconel with Cu interlayer b joint made without interlayer c joint with Cu interlayer

5 mm at a feed rate of 10 mm/min. Finally during forging stage, the rotating action of the rod held in the collet/spindle was stopped and was plunged into the stationary rod for 3 mm at a feed rate of 60 mm/min. Hence a total penetration of 8 mm (5 mm and 3 mm during friction and forging stages, respectively) was achieved.

The joints were tensile tested as per ASTM E8 standard at a strain rate of 10^{-3} /s and a crosshead speed of 2.16 mm/min on MTS landmark machine. The gauge length and gauge diameter of the tensile test samples was 36 mm and 9 mm, respectively. Samples for microstructural analysis were taken from the weld interface. These samples were polished with polishing papers (up to 2500 grit size), followed by electro polishing with an electrolyte consisting of ethanol, nitric acid, and propanol at 20 V and -10 °C for 20 s. Electron backscattered diffraction (EBSD) was performed on Gemini SEM 300 (Oxford detector) to analyze the base material's microstructure and joint interface. EBSD analysis was done with the Aztec HKL software with following parameters: scan area of $300 \mu\text{m} \times 300 \mu\text{m}$ and step size of $0.3 \mu\text{m}$. Upon tensile test, the fracture surfaces were examined by SEM imaging.

Results and Discussion

Microstructure of Joint Interface

The inverse pole figures (IPF) from EBSD of base material and the joint interface are shown in Fig. 3. On both sides of the interface, grain boundaries are considered for the misorientation angle greater than 10° and indicated by black color. Color coding used for IPF maps from EBSD is presented in Fig. 3e. From Fig. 3a, b, twin boundaries can be noticed in steel and Inconel, which impart high strength to these materials. The average grain size on Inconel side is $17.5 \mu\text{m}$ and the average grain size on steel side is $22 \mu\text{m}$. Figure 3c shows the IPF from EBSD of the joint interface for the joint made without Cu. The size of the grains on the steel side ($14.4 \mu\text{m}$) is smaller than the as-received SS 316L. The grain refinement on the steel side suggests dynamic recrystallization upon severe plastic deformation during the process. In contrast to the steel side, grain coarsening (grain size: $21.5 \mu\text{m}$) can be noticed on the Inconel side. The grain coarsening is attributed to the elevated temperatures due to frictional

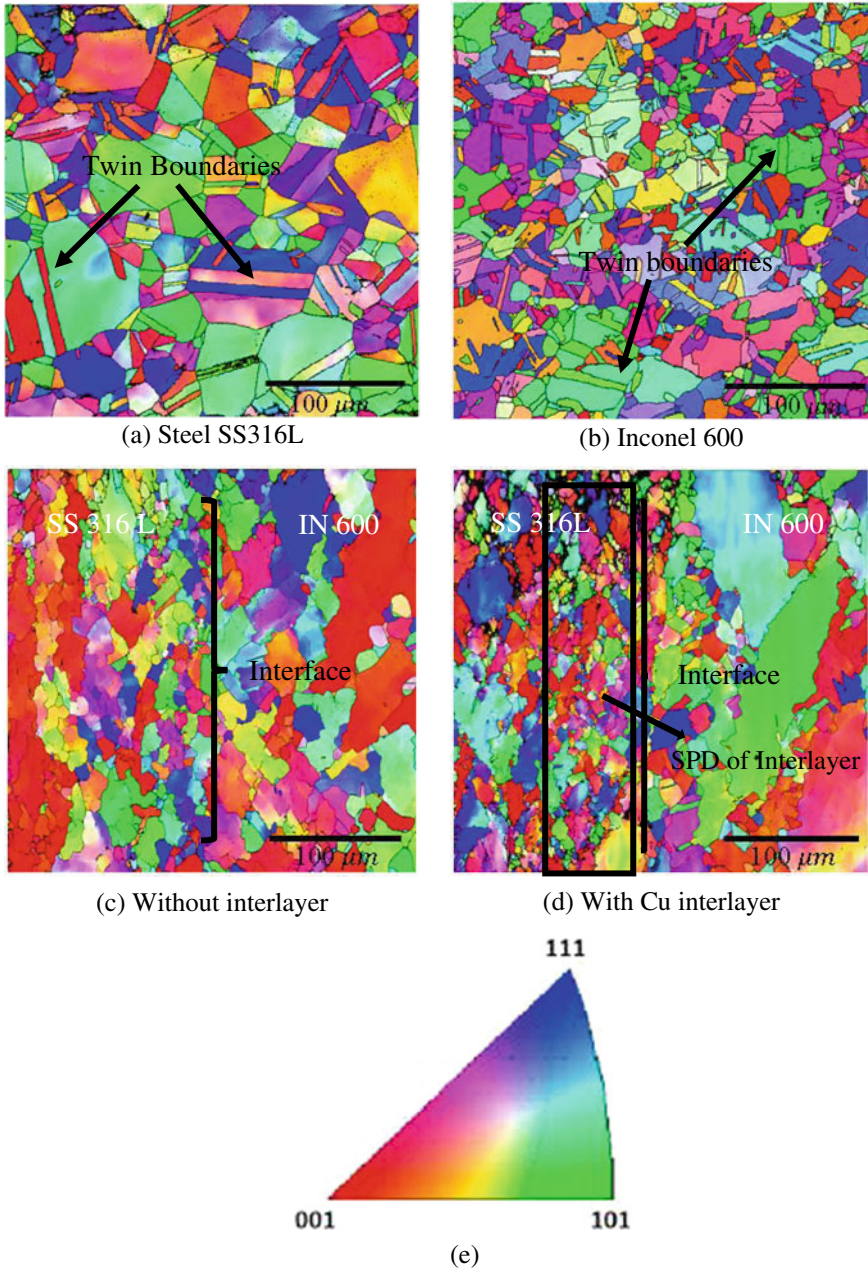


Fig. 3 EBSD IPF map of **a** Steel 316 L **b** Inconel 600 **c** joint without interlayer **d** joint with Cu interlayer and **e** color coding for IPF (FCC: γ -Fe, Cu and Ni) (Color figure online)

heating at the interface and dissipation form plastic deformation at the steel side. Figure 3d shows the IPF from EBSD of joint made with interlayer. Similar to the joint without interlayer, grain refinement is observed on the steel side. Also, the reduction in twin boundaries is noticed on both sides of the interface. Along with the steel near the interface, copper interlayer has also undergone severe plastic deformation. The corresponding region with very fine grains of average grain size of 4.2 μm at the interface is shown with a rectangular box in Fig. 3d. Relatively more grain growth (grain size: 46.6 μm) is observed on the Inconel side as compared against the joint without interlayer. This shows that the presence of Cu interlayer affects the grain growth on the Inconel side. The Inconel is subjected to temperature rise twice for the case of RFW with Cu interlayer: joining of Cu to Inconel and joining of SS 316L to Inconel with Cu interlayer.

Mechanical Properties and Fracture Analysis of Joints

The joint strength and ductility obtained by tension test along with base material properties are shown in Table 3. Three tension test samples were tested from each welded joint. The ultimate tensile strength (UTS) of joints with interlayer is 690.5 MPa which is 97.5% of the base material (SS316L) UTS. Percentage elongation i.e. ductility of the joint made with interlayer is 25.7%, against the base material (Inconel 600) ductility of 33%. The average UTS and % elongation of the joints made with interlayer are appreciably higher than the same for the joints made without interlayer.

The fracture surfaces from tension test samples are shown in Fig. 4. The circular marks on the fracture surface are attributed to the rubbing action between the work-pieces. From EDS analysis as expected, the presence of Fe, Cr and Ni was noticed on the steel side. The presence of Cu can also be seen in the joint made with Cu interlayer. This indicates that sticking between steel and Cu is achieved and Cu is uniformly distributed over the surface. The microvoids and coalescence of microvoids, i.e., dimples are present all over the fracture surface, particularly for the joint prepared with Cu interface, which indicates ductile failure upon tensile testing. For the joint

Table 3 Strength and ductility of the welded samples

Material	Ultimate tensile strength (UTS) (MPa)	Percentage elongation (%)
Base material Inconel 600	742	33
Base material steel 316L	708	46
In-steel joint (without interlayer)	623.3 ± 35	14.1 ± 3.3
In-Cu-steel joint (with Interlayer)	690.5 ± 17.7	25.7 ± 3.5

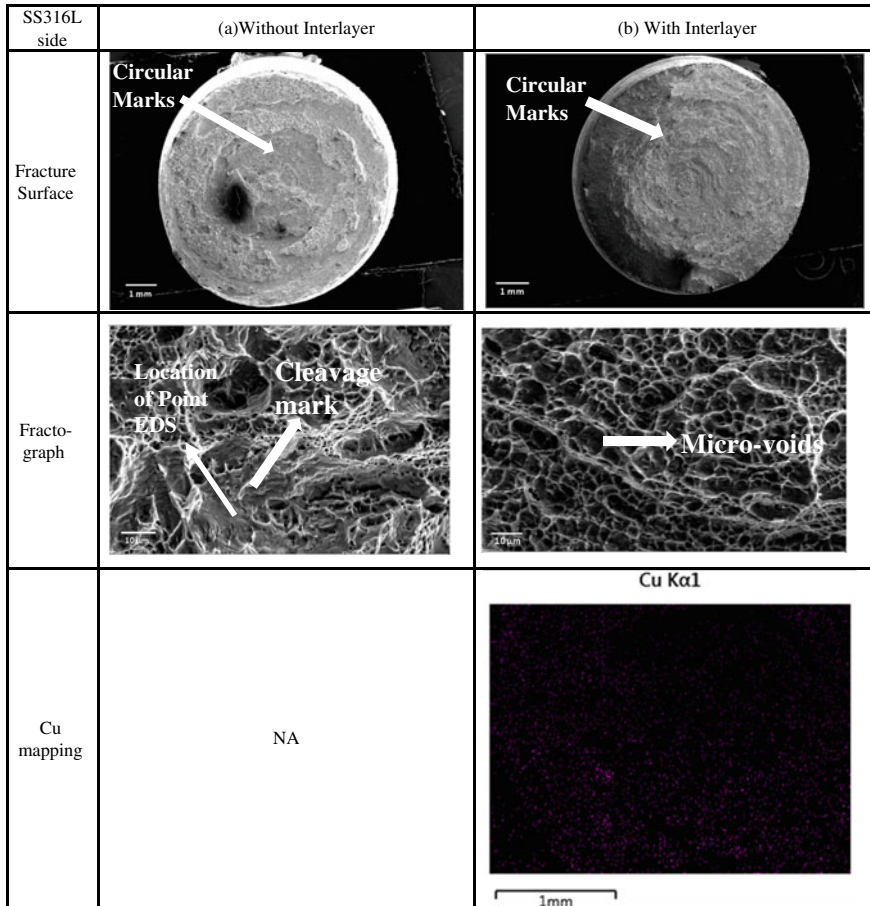


Fig. 4 Fracture surface and EDS Cu mapping of fracture surfaces from tension test of joints **a** without interlayer **b** with interlayer

prepared without interlayer, cleavage marks are noticed at few places on the steel side fracture surface from tension testing (Fig. 4). Point EDS at such a location revealed relatively high nickel content of about 32.6%, and 46.5% of Fe. This is suspected due to the formation of Fe–Ni intermetallics at these locations. The FeNi intermetallics were reported previously in the joints of Ni-based alloy K418 and 42CrMo steel [12]. The cleavage marks are not noticed on the fracture surface from the joints made with interlayer. This suggests that the Cu interlayer impeded the formation of Fe–Ni IMCs, which led to improvement of joint performance.

Conclusion

The current work focuses on the effect of Cu interlayer on the mechanical properties of the rotary friction welded joints of Inconel 600 and SS 316L steel. Joints were made at two different conditions: first, Inconel and steel were joined without interlayer, and second, Inconel and steel were joined with Cu interlayer. The RFW of Inconel 600 and SS 316L steel was performed at 3000 rpm at 10 mm/min feed rate during friction plunging stage and 60 mm/min feed rate during the forging stage. Based on the experimental investigation, following conclusions are drawn:

- (1) The joint strength and ductility of the joints with Cu interlayer are appreciably higher than the same for the joints made without interlayer. For both the joints, grain refinement on steel side and grain coarsening on Inconel side are noticed.
- (2) For the joints with Cu interlayer, fractography and EDS analysis of the fracture surface suggests sufficient sticking and uniform spreading of copper at the steel side, which would impede the formation of brittle Fe–Ni intermetallics. The presence of a sufficient amount of microvoids and dimples on the fracture surface suggests ductile fracture.
- (3) For joints without Cu interlayer, cleavage marks are noticed on the steel side fracture surface. The point EDS at the cleavage mark revealed significant presence of Ni on the steel side indicating Fe–Ni intermetallics, which would promote brittle fracture.
- (4) The joint efficiency of the joints made with Cu interlayer is 97.5% (w.r.t. SS316L) with percentage elongation of 25.7%, which also compares decently against the same for the base material (33% for Inconel 600).

References

1. Mortezaie A, Shamanian M (2014) An assessment of microstructure, mechanical properties, and corrosion resistance of dissimilar welds between Inconel 718 and 310S austenitic stainless steel. *Int J Press Vessels Pip* 116:37–46
2. Pavan AHV, Vikrant KSN, Ravibharath R, Singh K (2015) Development and evaluation of SUS 304H-IN 617 welds for advanced ultra-supercritical boiler applications. *Mater Sci Eng A* 642:32–41
3. Xu XY, Hong WANG, Zhang YE, Chang JW, Yao XU, Sun GA, Lü WJ, Gao YK (2019) Characterization of residual stresses and microstructural features in an Inconel 718 forged compressor disc. *Trans Nonferrous Metals Soc China* 29(3):569–578
4. Ramkumar KD, Sridhar R, Periwal S, Oza S, Saxena V, Hidad P, Arivazhagan N (2015) Investigations on the structure–property relationships of electron beam welded Inconel 625 and UNS 32205. *Mater Des* 68:158–166
5. Hernández M, Ambriz RR, Cortès R, Gómora CM, Plascencia G, Jaramillo D (2019) Assessment of gas tungsten arc welding thermal cycles on Inconel 718 alloy. *Trans Nonferrous Metals Soc China* 29(3):579–587
6. Sivakumar R, Mordike BL (1989) High temperature coatings for gas turbine blades: a review. *Surf Coat Technol* 37(2):139–160

7. Martin, DC, Miller FR (1972) Using solid-state joining in gas turbine engines. In: Turbo Expo: power for land, sea, and air, vol 79818. American Society of Mechanical Engineers, pp V001T01A073
8. Ahmad GN, Raza MS, Singh NK, Kumar H (2020) Experimental investigation on Ytterbium fiber laser butt welding of Inconel 625 and Duplex stainless steel 2205 thin sheets. *Opt Laser Technol* 126:106117.
9. Anandaraj JA, Rajakumar S, Balasubramanian V (2020) Investigation on mechanical and metal-lurgical properties of rotary friction welded In718/SS410 dissimilar materials. *Mater Today: Proc* 45(2):962–966
10. Rehman AU, Usmani Y, Al-Samhan AM, Anwar S (2021) Rotary Friction Welding of Inconel 718 to Inconel 600. *Metals* 11(2):244
11. Kangazian J, Shamanian M (2019) Microstructure and mechanical characterization of Incoloy 825 Ni-based alloy welded to 2507 super duplex stainless steel through dissimilar friction stir welding. *Trans Nonferrous Metals Soc China* 29(8):1677–1688
12. Ding Y, You G, Wen H, Li P, Tong X, Zhou Y (2019) Microstructure and mechanical properties of inertia friction welded joints between alloy steel 42CrMo and cast Ni-based superalloy K418. *J Alloy Compd* 803:176–184
13. Reddy GM, Ramana PV (2012) Role of nickel as an interlayer in dissimilar metal friction welding of Maraging steel to low alloy steel. *J Mater Process Technol* 212(1):66–77, 3036–3050.
14. Reddy MG, Rao SA, Mohandas T (2008) Role of electroplated interlayer in continuous drive friction welding of AA6061 to AISI 304 dissimilar metals. *Sci Technol Weld Joining* 13(7):619–628
15. Meshram SD, Reddy GM (2015) Friction welding of AA6061 to AISI 4340 using silver interlayer. *Def Technol* 11(3):292–298